

Received January 22, 2020, accepted February 7, 2020, date of publication February 17, 2020, date of current version February 27, 2020.

Digital Object Identifier 10.1109/ACCESS.2020.2974295

Systematic Design of a Parallel Robotic System for Lower Limb Rehabilitation

CALIN VAIDA¹, IOSIF BIRLESCU¹, ADRIAN PISLA¹, IONUT-MIHAI ULINICI¹,
DANIELA TARNITA², GIUSEPPE CARBONE^{1,3}, AND DOINA PISLA¹

¹CESTER, Technical University of Cluj-Napoca, 400020 Cluj-Napoca, Romania

²INCESA, University of Craiova, 200585 Craiova, Romania

³DIMEG, University of Calabria, 87036 Rende (CS), Italy

Corresponding author: Doina Pislă (doina.pisla@mep.utcluj.ro)

ABSTRACT This paper presents the design of an innovative robotic system for lower limb post-stroke rehabilitation of bed confined patients during the acute stage of the treatment. To establish the particularities of each targeted joint motion, experimental measurements are performed on healthy subjects. The acquired data is used to determine the operational workspace, namely the limits of the anatomic joints motion for the lower limb. Based on the prescribed operational workspace, an innovative parallel robotic architecture is designed for achieving the rehabilitation of the lower limb. A detailed kinematic modelling and analysis is carried out to demonstrate the robot capability to safely achieve the required motions. The design of the robotic rehabilitation device is discussed in detail alongside with numerical simulations for validating its performance while performing medically relevant rehabilitation motions.

INDEX TERMS Rehabilitation robotics, parallel robots, robot kinematics, modeling, numerical simulation, design engineering.

I. INTRODUCTION

In recent years stroke became the third most common cause of disability making up 4.5% of disability-adjusted life-years (DALYs) worldwide. Around 70% of stroke survivors experience some form of motor disability and must undergo a rehabilitation program [1], [2]. Post-stroke rehabilitation can be divided into three main phases: acute, sub-acute and chronic with the acute phase being the most effective for rehabilitation but also the most difficult to treat (see figure 1).

Robotic assisted rehabilitation devices have been widely addressed in the last decades with several existing design solutions [3]–[5]. Robotic rehabilitation devices for lower human limb can be classified as based on their structure as treadmill-based exoskeleton robots, leg orthoses, foot plate based devices and platform based devices. **Treadmill-based exoskeleton robots** are devices that use a harness-type support system to suspend the patient in an upright position. The LokoHelp [7] is such a device which uses the treadmill as an actuator, to guide the patient's legs along a set walking motion path. The patient is suspended via a harness mechanism and the leg is kept in the proper position via a leg

The associate editor coordinating the review of this manuscript and approving it for publication was Yangmin Li.

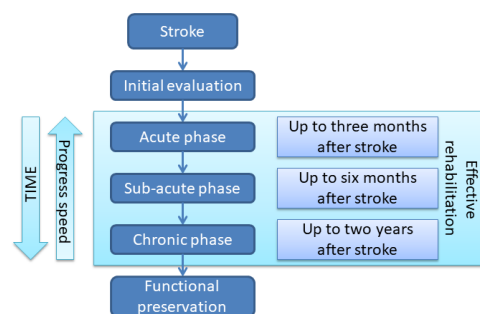


FIGURE 1. The post-stroke rehabilitation phases.

brace system. **Leg orthoses** and **exoskeleton** based structures, are robots that encompass the patient's affected limb or limb segments entirely [7] [8]. HAL or Hybrid Assistive Limb [9] is a wearable lower limb exoskeleton. Clinical and experimental studies on this device have shown that it can provide weight support and assist with activities of daily living (ADL). **Foot plate-based end effector systems**, are devices that guide the patient's limb from the foot upwards. Instead of having a joint based architecture, like exoskeletons, that require joint alignments between the device and the human limb, the device uses a footplate to move the leg by simulating foot movements, this in turn moving the other leg

joints accordingly. The Gait Trainer (GTI) [10] is a device that uses the movements of the lower limb to stimulate muscles and assist the patient in training. **Platform-based end-effector** devices are robotic systems that use a solution similar to that of a footplate, except these are generally made to exercise the different motions of the ankle joint, instead of simulating a walking pattern like footplate based structures. The Rutgers ankle [10], integrates features such as virtual reality, force feedback, and remote control. The mechanism consists of a mobile platform, a fixed platform and six double acting cylinders thus attaining 6 degrees of freedom (DOF).

Analyzing the existing devices for lower limb rehabilitation the authors identified a white spot in this field, namely the rehabilitation of bed-ridden patients, which cannot be treated in a vertical position. The aim of the paper is to present the systematic development a new robotic device that can be attached to the patient bed, performing rehabilitation exercises for the lower limb on all the major joints: hip, knee and ankle. The motivation of developing such robotic system emerges from the lack of existing solutions for severely disabled patients whom cannot stand, aiming to mobilize all the major joints of the lower limb. The challenges that should be overcome through the systematic design (consistent with the points addressed in [2] regarding robotic rehabilitation) are: the minimization of the active involvement of physical therapists (which should diminish the consequences of a predicted shortage in rehabilitation personnel [2]), the possibility to provide personalized treatment programs for each patient and the minimization of the production cost of the final robotic device.

Following the Introduction section the paper is structured as following: In Section II the proposed design approach is discussed; in Section III the motion intervals for each anatomic joint are deduced through experimental data obtained on healthy human subjects (the obtained motion intervals are the basis of the definition of the robot operational workspace); in Section IV a novel robotic system is proposed for lower limb rehabilitation specifically for bed ridden patients (in the acute treatment phase), where specific attention is addressed to kinematic modelling and singularity analysis which in turn are used to determine the operational workspace and validate the feasibility of the desired motion operations; in Section V the 3D CAD model is presented, designed in accordance to specific kinematic requirements discussed in previous sections and the mechanism components are detailed; in Section VI kinematic simulations are reported and discussed to illustrate the interaction between the active joint space and the human anatomic joints; the design of the robotic rehabilitation device is compared with other existing devices in (Section VII) - Discussion, showing some potential advantages and the conclusions are illustrated in Section VIII.

II. THE PROPOSED DESIGN APPROACH

A stepwise methodology for the development of a new, efficient robotic system for lower limb rehabilitation is

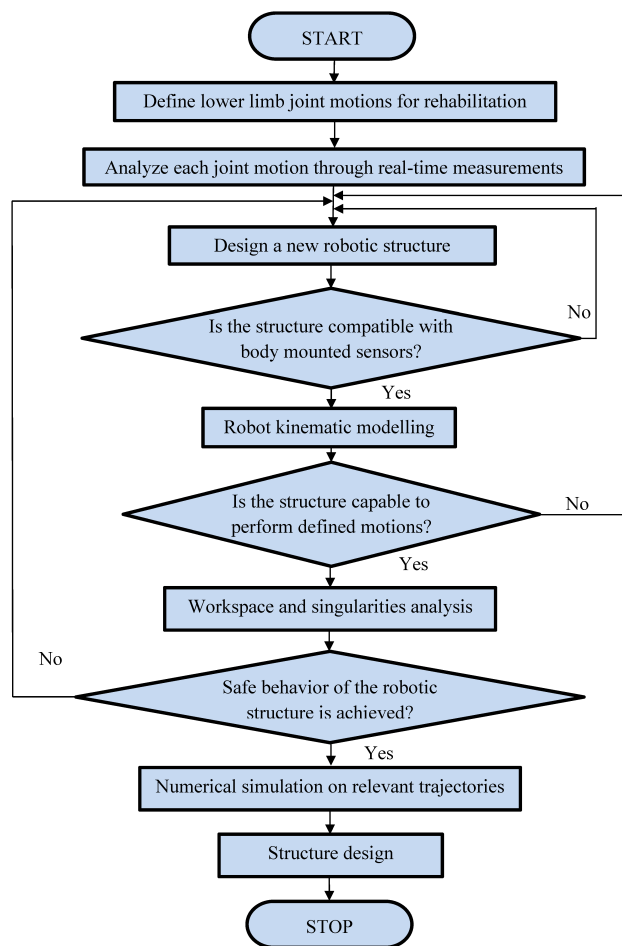


FIGURE 2. The stepwise process for the development of an efficient robotic system for rehabilitation.

presented in figure 2. The first step of this approach requires identifying the motions that have to be performed during a rehabilitation treatment, while a patient is lying on a bed. The next step requires identifying the motion amplitudes of each targeted anatomic joints [12], [13]. The motion amplitudes for each targeted anatomic joint (hip, knee and ankle) were analyzed using healthy subjects to determine the task (operating workspace) of the rehabilitation exercises (considering that the exercises start with lower amplitudes but they progress towards the values that describe healthy subjects). Using this information a new robotic structure can be designed integrating also the above defined sensors. The robot kinematic modelling will serve to define the control equations and, in parallel, the robot workspace and singularities.

In the next step, the safety of the robot is evaluated based on these findings as the robot should be able to reach the motion amplitudes defined (workspace) and to have a safe behavior (no singularities within the operational workspace). Using the equations from the kinematic modelling, in the next step numerical simulations of medically relevant exercises are performed to assess the robot behavior, followed by its 3D CAD design.

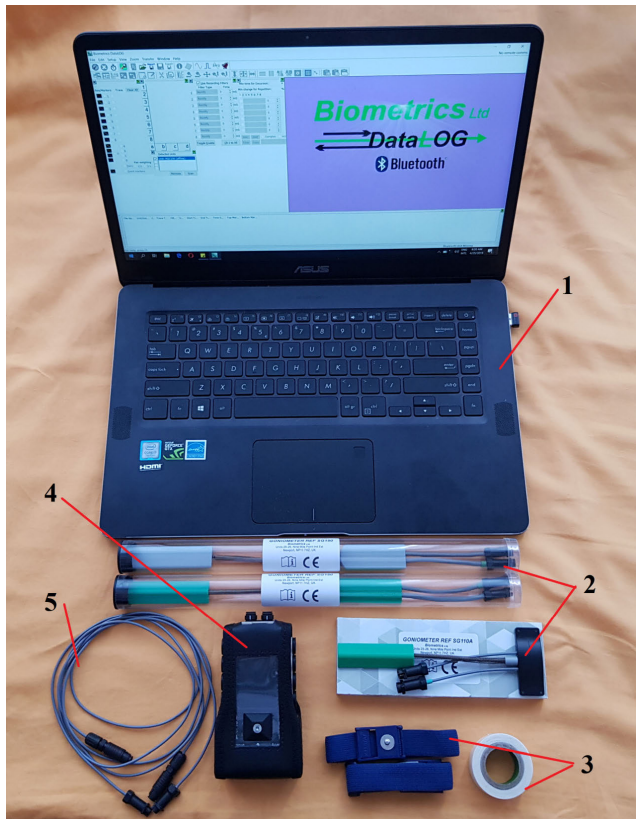


FIGURE 3. The components of the experimental bench.

III. JOINT MOTION ANALYSIS THROUGH EXPERIMENTAL MEASUREMENTS

For the systematic definition of the robotic device operational workspace the motion amplitudes for the targeted anatomic joints were determined using several healthy subjects. The motion data at this stage is used in order to define the functionality of the robotic system (considering that the amplitudes of motion are carefully increased with the progression of the patient to achieve motions close to the ones of healthy patients). The desired motions for the rehabilitation process (which represent also the subject of the experimental measurements) are:

(hip) - **flexion/extension and abduction/adduction;**

(knee) - **flexion/ extension;**

(ankle) - **dorsiflexion/plantar flexion and abduction/adduction.**

The authors have identified appropriate sensors used to measure directly the motion amplitudes and performed a series of experimental testing that aimed to evaluate:

- the motion amplitudes of healthy subjects which will be used to define the robot range for each targeted joint;
- the sensors behavior on different subjects with different anthropometric data;
- the sensors integration for real-time feedback in a rehabilitation system.

The sensors used during the experiments are provided by Biometrics having all the certifications required by biomedical applications [12]. For the experimental bench the following

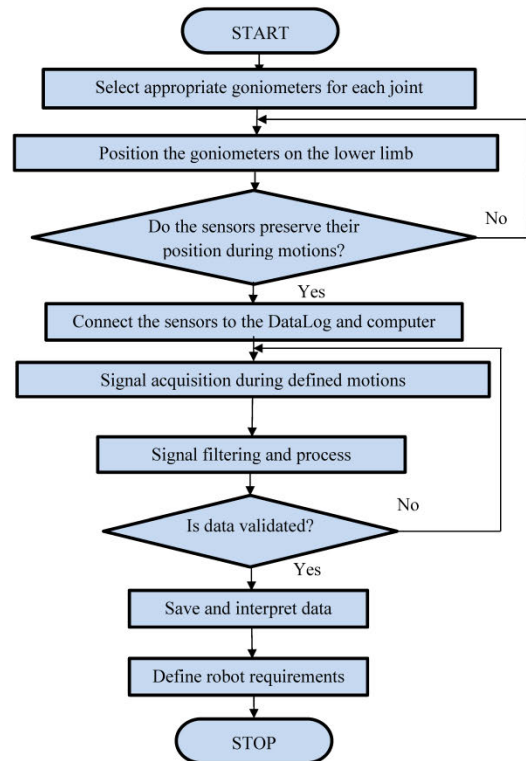


FIGURE 4. Experimental measurements diagram.

equipment is used (figure 3): (1) – mobile computer for signals processing; (2) – twin axes goniometers; (3) – medical grade adhesive tape and elastic bends; (4) – DataLog wireless signal transmission device; (5) – connection wires between goniometers and DataLog. Each goniometer can measure the motion amplitude in two perpendicular planes, enabling the study of the limb spatial trajectory when a specific motion is performed. The experimental process is synthesized in the diagram presented in figure 4.

Although there are far more precise technical solutions for tracking the anatomic joints motions, see for example the OptiTrack package [28] (which can track markers with precision better than 1 mm), or other camera based methods such as in [24], the authors opted to use the goniometers since in the rehabilitation process does not require a very high accuracy of the robotic device (as opposed to robots designed for percutaneous procedures such as biopsy and brachytherapy). As long as the goniometers are well calibrated their use for the rehabilitation is preferred (at least according to the kineto-therapists and medical personnel) since it is far easier to mount the sensors on the limb (than to mount the trackers and calibrate the camera tracking device which may be needed if the robot is moved in other place). Moreover, the described sensors' system (goniometers) will be part of the RAISE robotic system (to form closed loop control in order to ensure the patient safety) and their use is also intended for the patient evaluation in future stages of development (when the robotic system will be tested in hospital environment). Based

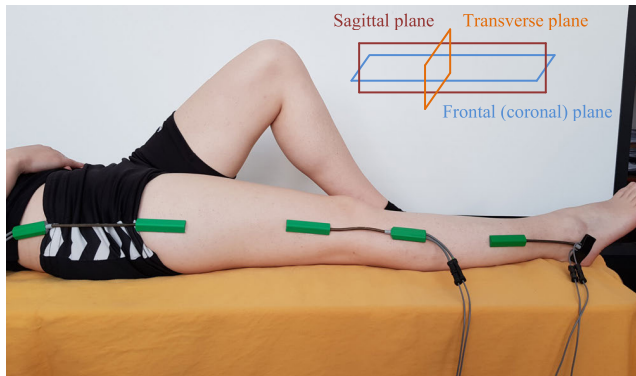


FIGURE 5. The positioning of the goniometers on the lower limb.

on the authors' clinical experience for upper limb rehabilitation [30], the general patient state imposes the use of sensors that can be mounted fast, easy and reliably with a simple setup. The experimental measurements were performed on 5 healthy subjects with the sensors positioned on the joints of the lower limb as shown in figure 5.

The experimental results are summarized in the next table and the signal processing is illustrated in a graphical form for one subject for each motion. All the signals recorded from the DataLog were processed in MATLAB, filtering the noise (third-order one-dimensional median filter), identifying the peaks in the signals and computing the relevant motion parameters.

The experimental measurements were performed as follows:

- each subject was requested to perform each motion by himself, to an amplitude which felt comfortable;
- each motion was performed with a number of 10 repetitions;
- for the hip, the flexion/extension was performed from the position presented in figure 5 requesting each subject to raise the leg in the sagittal plane;
- for the hip abduction/adduction each subject was asked to raise the leg to a low height in the sagittal plane, to perform 5 lateral motions (in the coronal plane) than to raise the leg to a different height and perform again 5 lateral motions;
- for the knee motions, each subject was asked to perform the flexion in the sagittal plane while keeping the knee in contact with the lying surface;
- for the ankle motions each subject was asked to perform the dorsiflexion/plantar flexion and afterwards the abduction/adduction.

The data presented in Table 1 represents the following:

(Hip): in case of Flexion/Extension the minimum, maximum, average, median and standard deviation of the amplitude peaks is computed;

in case of abduction/adduction, which has been measured at two different heights, the average values and the standard deviation is computed for the motions in the coronal plane (C) and Sagittal plane (S);

TABLE 1. Experimental data of the upper LIMB measurements.

Subject data								
Sbj.	Gender	Age	Weight [Kg]	Height [cm]				
1	Female	26	49.5	165				
2	Male	29	73	180				
3	Male	26	75	174				
4	Male	27	89	188				
5	Male	39	81	180				
HIP Motions [°]								
Flexion/Extension (Sagittal plane) Peaks								
Sbj.	Min	Max	Average	Median	Std			
1	55.26	61.83	57.99	58.05	1.98			
2	38.07	47.63	44.12	44.28	2.82			
3	42.98	56.42	48.03	47.14	3.89			
4	29.51	37.27	34.11	35.31	2.67			
5	46.91	61.02	53.92	53.03	4.37			
HIP Motions [°]								
Sbj.	Abd/Add (1)				Abd/Add (2)			
	AvgC	Std	AvgS	Std	AvgC	Std	AvgS	Std
1	13.3	3.16	30.39	3.58	17.9	5.2	40.93	1.68
2	27.29	1.26	16.74	2.16	23.16	4.19	34.73	4.77
3	6.67	1.01	20.52	2.68	6.85	1.71	27.23	1.08
4	14.83	3.49	11.13	2.07	10.23	1.34	17.17	1.93
5	16.07	2.19	31.83	1.37	34.08	2.01	53.34	2.25
KNEE Flexion/Extension Motions Peaks [°]								
Sbj.	Min	Max	Average	Median	Std			
1	108.02	110.39	109.57	109.63	0.6225			
2	94.77	102.89	98.41	97.35	2.7074			
3	115.66	117.62	116.38	117.37	0.6144			
4	96.19	99.41	97.71	97.96	0.9554			
5	122.84	126.28	124.13	123.89	1.1633			
ANKLE Motions Peaks [°]								
Sbj.	Dorsiflexion-plantar flexion				Adduction - Abduction			
	Avg.	Std.	Avg.	Std.	Avg.	Std.	Avg.	Std.
1	25.85	2.44	31.18	0.98	19.83	0.64	11.73	0.89
2	17.28	2.47	29.47	4.19	20.74	2.05	13.3	1.19
3	16.66	1.83	44.16	4.23	32.52	1.74	20.21	2.54
4	26.07	3.81	30.43	6.87	21.12	1.26	19.83	0.90
5	14.53	0.91	40.43	0.87	21.76	2.68	16.37	2.84

(Knee): for the knee flexion motions the minimum, maximum, average, median and standard deviation for the amplitude peaks are computed;

(Ankle): for each ankle motion the average values and the standard deviation for the amplitude peaks have been computed.

Figure 6 illustrates an example of the experimental data processed in MATLAB [17].

IV. RAISE – AN INNOVATIVE PARALLEL ROBOTIC SYSTEM FOR LOWER LIMB REHABILITATION

In [14] a novel parallel robotic system was introduced with the capability of mobilizing all the large joints of the lower limb following feasible ranges of motion: hip, knee and ankle. Based on the discussions with medical experts (kinetotherapists and neurologists) several enhancements were made:

- The total number of motions at the level of the lower limb has been increased;
- The motion amplitudes were extended to support a wider range of exercises;

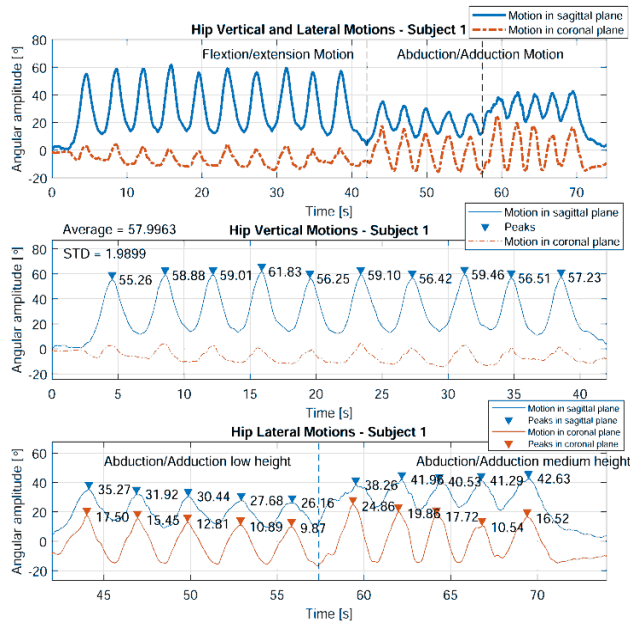


FIGURE 6. Motion curves for the hip motions of the human Subject 1.

TABLE 2. Motion ranges of raise robotic system.

	Flexion [°]	Extension[°]	Abduction[°]	Adduction[°]
Hip	~55	~0	~30	0
Knee	~80	0	-	-
Ankle	~35	~20	~20	~20

- The mechanical structure was designed to allow simple and accurate geometric variations based on the anthropometric patient data;
- The robot design was achieved in such a way to allow the use of two RAISE system side by side (mirrored) to allow the support for both limbs.

The motion capabilities (i.e. the operational workspace) of the new enhanced parallel structure - RAISE, are summarized, in terms of motion types and amplitudes in the Table 2. Regarding the motion amplitudes, for safety reasons, the maximum values are set below the capabilities of a “healthy person”, defined together medical experts using the experimental data presented in section III.

A. GEOMETRIC AND KINEMATIC MODELLING OF THE RAISE ROBOTIC SYSTEM

In order to develop the robotic system for rehabilitation the kinematics of the human lower limb must be considered. It is well established that the motions performed by the anatomic joints are far more complicated than simple rotations in basic mechanisms achieved via revolute or spherical joints (for the knee joint see for example [3]). However, the authors opted to use a simple kinematic model for the lower limb, namely the limb was approximated as being a URU kinematic linkage with a universal joint (U) describing the hip, a revolute joint (R) describing the knee and a universal joint (U) describing the ankle (only 2 degrees of freedom are intended for the rehabilitation of the ankle using the proposed robotic system).

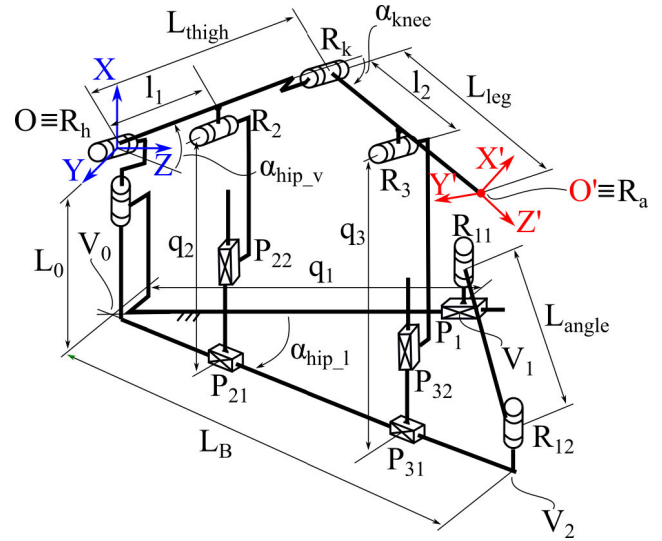


FIGURE 7. Kinematic scheme of the hip and knee rehabilitation module.

This simplification was possible due to the following reasons: i) the proposed robotic system contains a specific kinematic chain on which the lower limb is mounted (similarly to an exoskeleton) with its mechanical joints placed adjacent, or as close as possible, to the anatomic human joints; ii) the lengths of the links of the kinematic chain on which the limb is mounted are adjustable to create modularity (i.e. adjust to anthropometric variations), therefore the alignment of the mechanical joints with the anatomical joints is achievable; iii) the anchor elements placed on the RAISE robotic system are compliant (there is no fixture between the anchor elements of the mechanism with the lower limb segments), therefore during the rehabilitation exercises the lower limb is not forced into specific motions that may produce injury. The reasoning of choosing this simple kinematic model for the lower limb is also discussed in [29].

The initial conceptual solution for the RAISE robotic system was designed with 4 DoF (degrees of freedom), achieved using two coupled rehabilitation modules. The first module was a 2 DoF planar parallel mechanism, targeting the flexion/extension of the hip and knee joints; and the second module was a 2 DoF spherical mechanism, targeting the flexion/extension and adduction/abduction of the ankle joint.

The mechanism was slightly redesigned to extend its functionality, but the modularity of the system was kept. A third DoF was added for the hip and knee rehabilitation module, namely the hip abduction/adduction. Consequently, the **hip and knee rehabilitation module** became a 3 DoF parallel spatial mechanism (Fig. 7), while the ankle module remained a spherical 2 DoF RR mechanism (Fig. 8).

Having the kinematic schemes of the two modules of the robot the structural synthesis can be achieved using the formula derived by Plitea [15]:

$$M = (6 - F) \cdot N - \sum_{i=1..5} (i - F) \cdot C_i, \quad i = 1..5 \quad (1)$$

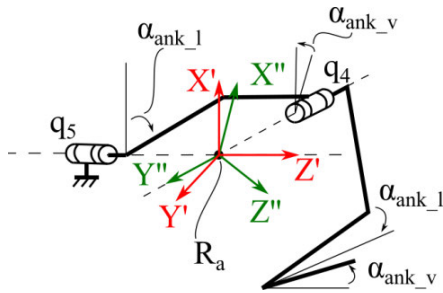


FIGURE 8. Kinematic scheme of the ankle rehabilitation module.

where: M – represents the degree of mobility for the mechanism; F – the mechanism family (defined as the total number of common constraints for all the mechanism elements which respect to the 6 possible motions in space), N – the number of mobile elements and C_i – the number of joints of i -class (where the class is defined as the number of motion restrictions introduced by a joint – e.g. a revolute joint is of class 5, a spherical joint is of class 3). A further condition imposes that all the terms should be positive. For the **hip and knee rehabilitation module**, the numerical values of the parameters in (1) and hence, the degree of mobility is:

$$F = 3, \quad N = 9, \quad C_5 = 12 \Rightarrow M = 3 \quad (2)$$

Thus the mobility degree of the first module is three, corresponding to the number of independent motions that will be performed with it. For the **ankle rehabilitation module** the degree of mobility is:

$$F = 2, \quad N = 3, \quad C_5 = 4 \Rightarrow M = 2 \quad (3)$$

To derive the geometric and kinematic models a set of coordinate frames were introduced (both fixed and mobile). Firstly, for the hip and knee rehabilitation module, the $OXYZ$ coordinate frame is a fixed one with its origin coincident with the intersection axes of the universal joint R_h (see Figure 7), and $O'X'Y'Z'$ is a mobile coordinate frame with its origin at the ankle rotation point R_a . Secondly, for the ankle rehabilitation module, the $O'X'Y'Z'$ serves as a fixed coordinate frame (as the two rehabilitation modules are coupled together) while $O''X''Y''Z''$ is a mobile one, both having the origin R_a (Figure 8).

The kinematic model of RAISE enables the definition of the motion equations at the level of each actuator for the generation of medically relevant trajectories for the targeted joints of the lower limb.

For the kinematic modeling of RAISE, Table 3 introduces a set of notations for the geometrical parameters of the structure.

To describe the motion of the hip and knee rehabilitation module four kinematic chains are defined as follows:

1. The **first kinematic chain** is a UR linkage with all the three rotation motions being free. It starts at the rotation axes intersection of the universal joint R_h (or the origin of the fixed coordinate frame) and ends at the point R_a (or the origin of the moving coordinate frame).

TABLE 3. The geometric parameters of the raise robotic structure.

Parameter	Description
α_{hip_v}	The angle value at the level of the hip joint - flexion/extension
α_{hip_l}	The angle value for the lateral motion of the lower limb, from the hip joint - abduction/adduction
α_{knee}	The angle between the thigh and the leg - flexion
α_{ank_v}	The input angle values for the ankle flexion/extension
α_{ank_l}	The input angle values for the ankle adduction/abduction
l_1	The distance between the revolute joints R_h and R_1
l_2	The distance between the revolute joints R_k and R_2
L_{high}	The distance between the revolute joints R_h and R_k
L_{leg}	The distance between the revolute joints R_k and R_a
L_{angle}	The distance between the revolute joints R_{11} and R_{12}
L_B	The distance between the axis of the revolute joint R_{12} and the OX axis
L_0	The distance along the OX axis between the origin of the fixed coordinated system and the plane $P_1P_{21}P_{31}$
q_i	The value of the “ i ” active joint
\dot{X}	The vector of the velocities of the input angles: $\dot{X} = [\dot{\alpha}_{hip_l} \quad \dot{\alpha}_{hip_v} \quad \dot{\alpha}_{knee} \quad \dot{\alpha}_{ank_v} \quad \dot{\alpha}_{ank_l}]^T$
\dot{Q}	The vector of the velocities of the active joints: $\dot{Q} = [\dot{q}_1 \quad \dot{q}_2 \quad \dot{q}_3 \quad \dot{q}_4 \quad \dot{q}_5]^T$
\ddot{X}	The vector of the accelerations of the input angles: $\ddot{X} = [\ddot{\alpha}_{hip_l} \quad \ddot{\alpha}_{hip_v} \quad \ddot{\alpha}_{knee} \quad \ddot{\alpha}_{ank_v} \quad \ddot{\alpha}_{ank_l}]^T$
\ddot{Q}	The vector of the accelerations of the active joints: $\ddot{Q} = [\ddot{q}_1 \quad \ddot{q}_2 \quad \ddot{q}_3 \quad \ddot{q}_4 \quad \ddot{q}_5]^T$

This UR linkage actually serves as an exoskeleton which guides the trained limb using anchor elements which are mounted on the mechanism links (see Section V);

- The **second kinematic chain** is a PRR chain with one active linear motion (actuated by q_1 through the prismatic joint P_1) along an axis parallel with OZ of the fixed frame, and two free rotation motions (through the revolute joints R_{11} and R_{12}) around axes parallel to the OX axis. Actuating this kinematic chain varies the angle α_{hip_l} which in turn produces the abduction/adduction on the hip;
- The **third kinematic chain** is a PPR chain with: one free linear motion (through the prismatic joint P_{21}) on a horizontal direction (in the OYZ plane of the fixed coordinate frame); one active linear vertical motion (actuated by q_2 through the prismatic joint P_{22}) along an axis parallel with the OX axis of the fixed frame; one free rotation motion around an axis parallel with the OYZ plane through the revolute joint R_2 (which is linked with the first kinematic chain). Actuating this kinematic chain will change the angle α_{hip_v} which in turn produces the flexion/extension of the hip;
- The **forth kinematic chain** is identical with the third one. It is a PPR chain with one free linear motion

(see above) through the prismatic joint P_{31} , one active linear vertical motion (actuated by q_3 through the prismatic joint P_{32}), and one free rotation through the revolute joint R_3 (which is also linked with the first kinematic chain). Actuating this kinematic chain will change the angle α_{knee} which in turn produces the flexion/extension of the knee (while q_2 remains constant that is).

Since different patients may have different limb segment lengths (referred to as anthropomorphic variables), the total lengths of L_{thigh} and L_{leg} must also be adjustable. A possible solution is to allow the lengths l_1 and l_2 to be adjustable before the rehabilitation exercises. The design of the robotic system accounts for the anthropomorphic variables (further details are presented in Section V).

The **ankle rehabilitation module** (Figure 8) is an **RR** mechanism with spherical architecture actuated by the active joints q_4 and q_5 . Through the actuation of q_4 the angle α_{ank_l} varies which in turn produces the abduction/adduction of the ankle joint. Furthermore, through the actuation of q_5 , the angle α_{ank_v} changes which induces the flexion/extension motion of the ankle.

In order to solve the kinematic model for RAISE, one must underline that, in the rehabilitation process, the kinetherapist which sets up the exercises will never configure the robot based on the coordinates of certain points of interest but rather by setting angular amplitudes for the parameters which correspond to the motions of the lower limb. Thus, in the kinematic model, the authors will determine the equations that establish a relationship between these angles and the values of the active joints. For the first active joint (q_1) can be calculated using the law of cosines in the triangle $V_0V_1V_2$ where the lengths of the two sides are known as fixed geometric coordinates and the angle $V_0V_1V_2$ as input parameter. From the two corresponding solutions, knowing that the angle must be lower than $\pi/2$ the smaller value is used, thus:

$$q_1 = L_B \cdot \cos(\alpha_{hip_l}) - \sqrt{L_B^2 \cdot \cos(\alpha_{hip_l})^2 - L_B^2 + L_{angle}^2} \quad (4)$$

The second active joint is:

$$q_2 = L_O + l_1 \cdot \sin(\alpha_{hip_v}) \quad (5)$$

The coordinates of the point R_k are:

$$\begin{cases} X_{Rk} = L_{thigh} \cdot \sin(\alpha_{hip_v}) \\ Y_{Rk} = L_{thigh} \cdot \cos(\alpha_{hip_v}) \cdot \sin(\alpha_{hip_l}) \\ Z_{Rk} = L_{thigh} \cdot \cos(\alpha_{hip_v}) \cdot \cos(\alpha_{hip_l}) \end{cases} \quad (6)$$

Moving on to the knee, the coordinates of the point R_3 have the following expressions:

$$\begin{cases} X_{R_3} = X_{Rk} + l_2 \cdot \sin(\alpha_{hip_v} + \alpha_{knee}) \\ Y_{R_3} = Y_{Rk} + l_2 \cdot \cos(\alpha_{hip_v} + \alpha_{knee}) \cdot \sin(\alpha_{hip_l}) \\ Z_{R_3} = Z_{Rk} + l_2 \cdot \cos(\alpha_{hip_v} + \alpha_{knee}) \cdot \cos(\alpha_{hip_l}) \end{cases} \quad (7)$$

Thus, the coordinates of the third active joint are:

$$q_3 = L_O + L_{thigh} \cdot \sin(\alpha_{hip_v}) + l_2 \cdot \sin(\alpha_{hip_v} + \alpha_{knee}) \quad (8)$$

The coordinates of the ankle joint, R_a are:

$$\begin{cases} X_{Ra} = X_{Rk} + L_2 \cdot \sin(\alpha_{hip_v} + \alpha_{knee}) \\ Y_{Ra} = Y_{Rk} + L_2 \cdot \cos(\alpha_{hip_v} + \alpha_{knee}) \cdot \sin(\alpha_{hip_l}) \\ Z_{Ra} = Z_{Rk} + L_2 \cdot \cos(\alpha_{hip_v} + \alpha_{knee}) \cdot \cos(\alpha_{hip_l}) \end{cases} \quad (9)$$

The last two active coordinates, based on the fact that the second module is a spherical one, have simple expressions:

$$q_4 = \alpha_{ank_v} \quad (10)$$

$$q_5 = \alpha_{ank_l} \quad (11)$$

Using (4) ÷ (11), the implicit functions of the mechanism can be defined, in order to compute the Jacobi matrices A and B. Thus a system of five equations can be written:

$$\begin{aligned} f_1 &: q_1 - L_B \cos(\alpha_{hip_l}) + \sqrt{L_B^2 \cos(\alpha_{hip_l})^2 - L_B^2 + L_{angle}^2} \\ f_2 &: q_2 - L_O - l_1 \sin(\alpha_{hip_v}) \\ f_3 &: q_3 - L_O - L_{thigh} \sin(\alpha_{hip_v}) - l_2 \sin(\alpha_{hip_v} + \alpha_{knee}) \\ f_4 &: q_4 - \alpha_{ank_v} \\ f_5 &: q_5 - \alpha_{ank_l} \end{aligned} \quad (12)$$

The A Jacobi matrix which represents the partial derivatives of the five implicit functions with respect to the input parameters, namely the five angles of interest will have to following expression:

$$A = \begin{bmatrix} A_{11} & 0 & 0 & 0 & 0 \\ 0 & A_{22} & 0 & 0 & 0 \\ 0 & A_{32} & A_{33} & 0 & 0 \\ 0 & 0 & 0 & -1 & 0 \\ 0 & 0 & 0 & 0 & -1 \end{bmatrix} \quad (13)$$

where:

$$\begin{aligned} A_{11} &= -\sin(\alpha_{hip_h}) L_B - \frac{\cos(\alpha_{hip_l}) L_B^2 \sin(\alpha_{hip_l})}{\sqrt{L_B^2 \cos(\alpha_{hip_l})^2 - L_B^2 + L_{angle}^2}} \\ A_{22} &= -\cos(\alpha_{hip_v}) l_1 \\ A_{32} &= \cos(\alpha_{hip_v}) L_{thigh} - \cos(\alpha_{hip_v} + \alpha_{knee}) l_2 \\ A_{33} &= -\cos(\alpha_{hip_v} + \alpha_{knee}) l_2 \end{aligned}$$

The second Jacobi matrix, B, is obtained calculating the partial derivatives of the implicit functions (12) with respect to the active coordinates. Thus, the B matrix is a 5×5 identity matrix.

The kinematic model for velocities is calculated using the well-known matrix identity between the velocities of the input angles and the ones of the active joints [16]:

$$A \cdot \dot{X} + B \cdot \dot{Q} = 0 \quad (14)$$

Considering that the input values for the velocities of the joint angles are known it results:

$$\dot{Q} = -B^{-1} \cdot A \cdot \dot{X} \quad (15)$$

The analytical expressions for the five active joints velocities are:

$$\begin{aligned} \dot{q}_1 &= \frac{-\sin(\alpha_{hip_l})L_B - \cos(\alpha_{hip_l})L_B^2 \sin(\alpha_{hip_l})}{\sqrt{\cos(\alpha_{hip_l})^2 L_B^2 + L_{angle}^2}} \dot{\alpha}_{hip_l} \\ \dot{q}_2 &= \cos(\alpha_{hip_v}) l_1 \dot{\alpha}_{hip_v} \\ \dot{q}_3 &= [\cos(\alpha_{hip_v}) L_{thigh} + \cos(\alpha_{hip_v} + \alpha_{knee}) l_2] \\ &\quad \cdot \dot{\alpha}_{hip_v} + \cos(\alpha_{hip_v} + \alpha_{knee}) l_2 \dot{\alpha}_{knee} \\ \dot{q}_4 &= \dot{\alpha}_{ank_v} \\ \dot{q}_5 &= \dot{\alpha}_{ank_l} \end{aligned} \quad (16)$$

The time derivative of (14) leads to the following matrix expression:

$$A \cdot \ddot{X} + \dot{A} \cdot \dot{X} + B \cdot \ddot{Q} + \dot{B} \cdot \dot{Q} = 0 \quad (17)$$

Considering as known the values for the joint angles accelerations, from (17) it results:

$$\ddot{Q} = -B^{-1} \cdot (A \cdot \ddot{X} + \dot{A} \cdot \dot{X} + \dot{B} \cdot \dot{Q}) \quad (18)$$

Introducing the following notations:

$$\begin{aligned} A_a &= \cos(\alpha_{hip_l}) \cdot L_B^2 - L_B^2 + L_{angle}^2 \\ w_1 &= -\frac{\cos(\alpha_{hip_l})L_B - \cos^2(\alpha_{hip_l})L_B^4 \sin^2(\alpha_{hip_l})}{\sqrt{A_a^3}} \\ &\quad - L_B^2 \frac{\sin^2(\alpha_{hip_l}) - \cos^2(\alpha_{hip_l})}{\sqrt{A_a}} \\ w_2 &= \frac{-\sin(\alpha_{hip_l})L_B + \cos(\alpha_{hip_l})L_B^2 \sin(\alpha_{hip_l})}{\sqrt{A_a}} \end{aligned} \quad (19)$$

The analytic expressions of the five equations that characterize the accelerations of the active joints are:

$$\begin{aligned} \ddot{q}_1 &= w_1 \cdot \dot{\alpha}_{hip_l}^2 + w_2 \cdot \ddot{\alpha}_{hip_l} \\ \ddot{q}_2 &= -\sin(\alpha_{hip_v}) l_1 \dot{\alpha}_{hip_v}^2 + \cos(\alpha_{hip_v}) l_1 \ddot{\alpha}_{hip_v} \\ \ddot{q}_3 &= -\sin(\alpha_{hip_v}) L_{thigh} \dot{\alpha}_{hip_v}^2 \\ &\quad - \sin(\alpha_{hip_v} + \alpha_{knee}) l_2 (\dot{\alpha}_{hip_v} + \dot{\alpha}_{hip_l})^2 \\ &\quad + (\cos(\alpha_{hip_v}) L_{thigh} + \cos(\alpha_{hip_v} + \alpha_{knee}) l_2) \dot{\alpha}_{hip_l} \\ &\quad + \cos(\alpha_{hip_v} + \alpha_{knee}) l_2 \ddot{\alpha}_{knee} \\ \ddot{q}_4 &= \ddot{\alpha}_{ank_v} \\ \ddot{q}_5 &= \ddot{\alpha}_{ank_l} \end{aligned} \quad (20)$$

B. SINGULARITIES ANALYSIS AND WORKSPACE GENERATION FOR THE RAISE ROBOTIC SYSTEM

A simple way to study the singularities of the mechanism is to evaluate the vanishing points of determinants of the Jacobi matrices. While in the case of matrix B the determinant is 1, the determinant of matrix A has the following expression:

$$\begin{aligned} \det(A) &= \sin(\alpha_{hip_l}) L_B \cos(\alpha_{hip_v}) l_1 \cdot \cos(\alpha_{hip_v} + \alpha_{knee}) \\ &\quad \times l_2 \left[1 - \frac{\cos(\alpha_{hip_l}) \cdot L_B}{\sqrt{\cos(\alpha_{hip_l})^2 \cdot L_B^2 + L_{angle}^2}} \right] \end{aligned} \quad (21)$$

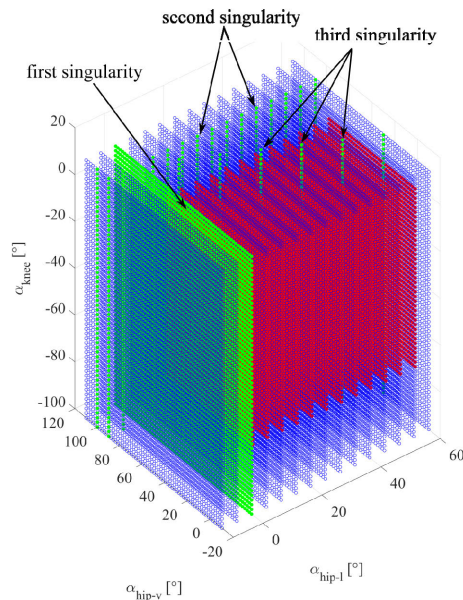


FIGURE 9. Hip and Knee module workspace.

From (21) there are three cases when the determinant of matrix A vanishes, as the remaining factors have always values greater than 0:

1. $\sin(\alpha_{hip_l}) = 0 \Leftrightarrow \alpha_{hip_l} = 0$ - **the first singularity** would correspond to the case when the leg is straight meaning that the robot would start in a singular position; in the CAD design, which is the subject of the next section a distancing element was introduced to avoid this singularity which was thus eliminated;

2. $\cos(\alpha_{hip_v}) = 0 \Leftrightarrow \alpha_{hip_v} = \pm\pi/2$ - **the second singularity** corresponds with the case when the thigh is lifted with 90° in either direction, but this value is outside the motion amplitudes imposed by the medical experts so this singularity condition is outside the operational (task) workspace;

3. $\cos(\alpha_{hip_v} + \alpha_{knee}) = 0 \Leftrightarrow \alpha_{hip_v} + \alpha_{knee} = \pm\pi/2$ - **the third singularity** corresponds with the case when the lower segment of the limb is vertical (parallel with the OX axis of the fixed coordinate system), which introduces a condition that has to be avoided within the operational workspace of the robot.

C. WORKSPACE

For the workspace analysis, a mapping has been done to study the correspondence between the values of the input angles and the values of the active joints for the hip-knee module, illustrated in Figure 9.

The red points represent the values of the input angles with the limits defined in Table 2. The blue points represent values outside those limits, while the green points represent singular configurations. These plots illustrate that only the third singularity is present within the operational workspace of the robot.

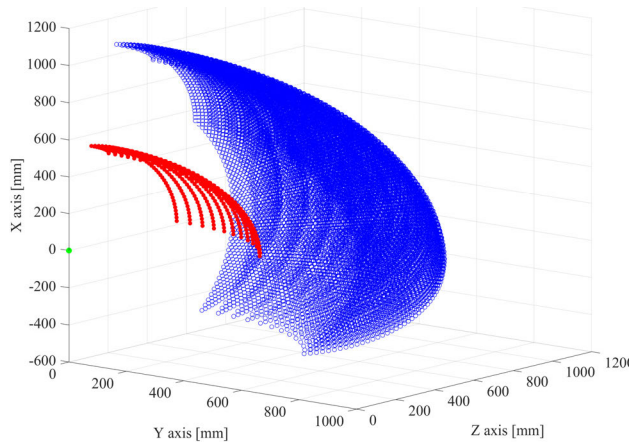


FIGURE 10. Hip and Knee module operational workspace.

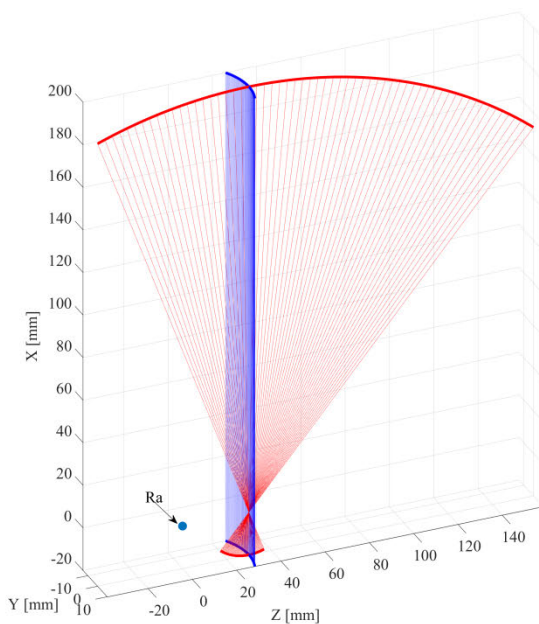


FIGURE 11. The operational workspace for the ankle module.

Figure 10 represents the hip-knee workspace determined as a point cloud with values varying between the limits defined in Table 2, while Figure 11 represents the workspace of the ankle module (red line - dorsiflexion/plantar flexion and blue line adduction/abduction) which based on the equations of the Jacobi determinants is singularity free.

V. CAD MODELLING OF RAISE

The robotic system (Figure 12.a) has two coupled modules (first for the hip/knee exercises and the second for the ankle exercises) mounted on a wheeled-frame to facilitate the device transportation. The anchor parts placed on the UR exoskeleton, and on the ankle module allow the mounting of the lower limb.

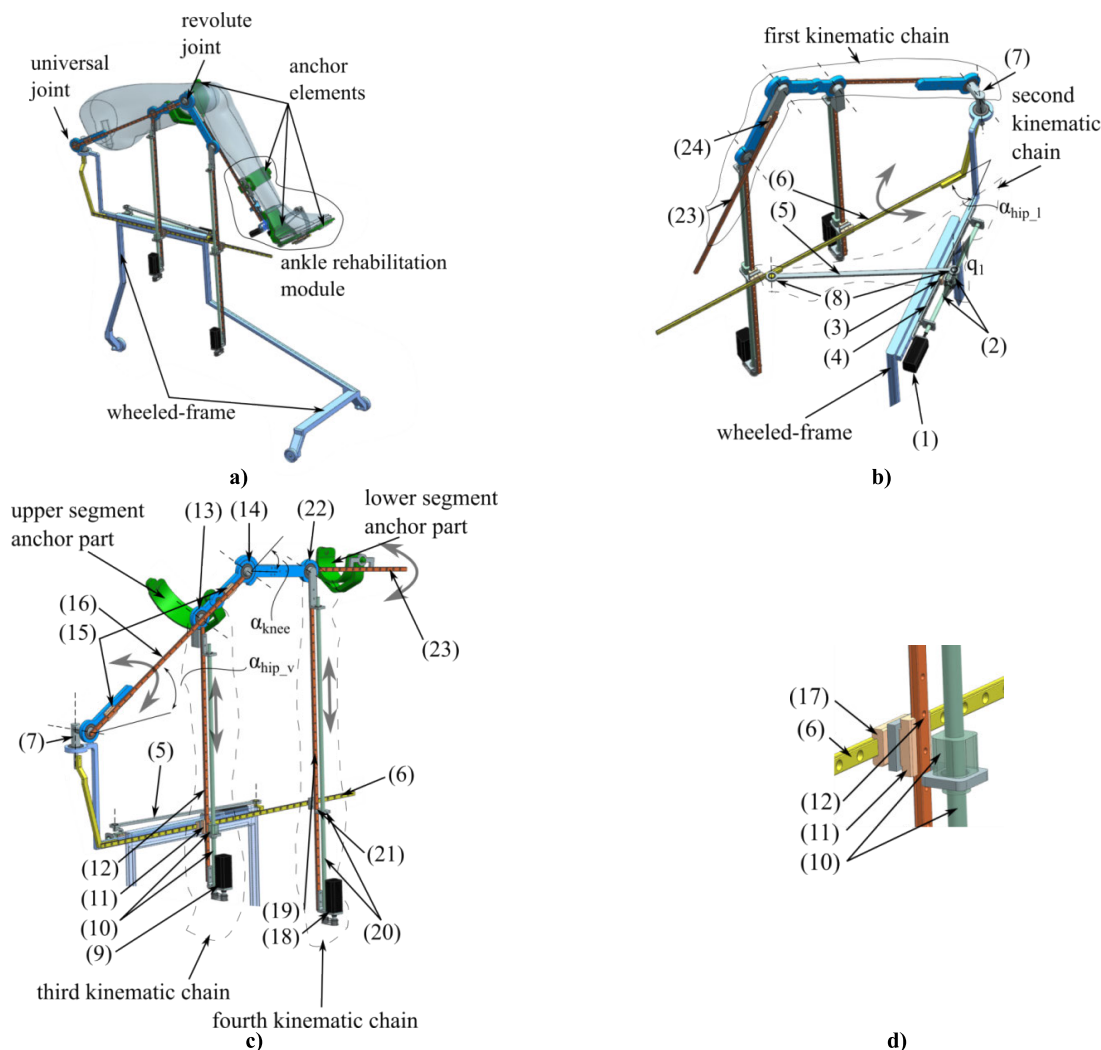
The *second kinematic chain* actuated q_1 (illustrated in detail in Figure 12.b), performs the hip adduction/abduction

motion by guiding the first kinematic chain as following; under the actuation of the rotary motor (1), the (ball) screw/nut mechanism (2) produces linear motion on the sledge (3) which slides on the rail (4). The motion of the sledge (3) produces in turn the change in the α_{hip_1} angle, since the link (5) moves the rail-frame (6) around the vertical rotation axis of the universal joint (7). The link (5) consequently has at its extremities two revolute joints (8).

The motion of hip flexion/extension (by varying the α_{hip_v}) is performed under the actuation of q_2 (through the third kinematic chain illustrated in Figure 12.c), which induces linear motion from a rotatory motor (9) through a (ball) screw/nut mechanism, towards a sledge (11) (attached to the nut) which slides on a rail (12). The upper extremity of the rail (12) forms a revolute joint (13) with the link between the universal joint (7) (aligned with the hip) and the revolute joint (14) (aligned with the knee). The length of the link is adjustable before the exercises (to compensate the anthropomorphic variations) since the sledges (15) can be slid on the rail (16) adjusting the distance between the universal joint (7) and the revolute joint (14). The mechanical element that links the revolute joints (13) and (14) also has the anchor part for the upper segment of the lower limb (using also a revolute joint to allow the free rotation motion of the anchor element for compliance reasons to avoid trauma on the patients limb).

For the hip flexion/extension motion, while the rail (12) is lifted (or lowered), the rail must also slide horizontally (since the revolute joint (14) is constrained to move in a circle around the horizontal rotation axis of the universal joint (7)). To achieve the horizontal motion of the rail (12), an assembly of two sledges mounted back to back is used (with perpendicular linear motion directions as illustrated in Figure 12.d). The assembly contains the sledge (11) with the rail (12) sliding through it (actuated by (9)), and a second sledge (17) sliding on the rail (6) (as a free linear motion). The motion of the knee flexion/extension is performed by a combination of both the active (prismatic) joints q_2 and q_3 (through the **third** and **fourth kinematic chains** illustrated in Figure 12.c). The fourth kinematic chain functions exactly like the third one, with the rotary motion from the motor (18) inducing a linear motion on the rail (19) (through a screw/nut (20)) which slides vertically through a sledge (21). Similarly with the third kinematic chain (actuated by q_2 with the motor (9)), the rail (19) forms a revolute joint (22) at its upper extremity.

While the rail (19) is slid up and down, the angle α_{knee} between links connected into the revolute joint (14) (adjacent to the knee) changes (provided that the motor (9) is not actuated). Just like in the third kinematic chain, a horizontal motion of the rail (19) is necessary (since the revolute joint (22) is constrained to move on a circular path around the revolute joint (14)). The same approach with an assembly with two back to back sledges was used, the first allowing the actuated linear motion of the rail (19) through the rail (21), and the second one sliding freely on the rail (6).



a) the two rehabilitation modules (hip/knee and ankle); b) the second kinematic chain of the hip and knee rehabilitation module; c) the third and fourth kinematic chains of the hip and knee rehabilitation module; d) back to back cross sledge assembly.

FIGURE 12. RAISE rehabilitation robotic system (CAD representation).

The anchor parts for the lower segment of the limb are mounted on the rail (23) also using a revolute joint for compliance reasons (to avoid trauma during the rehabilitation exercises). The rail (23) is mounted on the sledge (24) which allows the length variation of the exoskeleton link adjacent to the lower segment of the patients' limb (before starting the rehabilitation exercises).

As illustrated in Figure 16, the ankle rehabilitation module is spherical mechanism, mounted on the rail (23) through the frame (a). For the adduction/abduction motion, the frame (a) has the rotatory motor (b) mounted, which rotates a second frame (c) around an anteroposterior axis. Furthermore, the frame (c) has the second rotatory motor (d) mounted, which produces rotation motion around a mediolateral axis of the link (e) (through pulleys and a timing belt). The sole support (f) is linked with (e) at the inferior extremity through a rail/sledge mechanism (g). This is to allow compliance for the rehabilitation exercises (as the center of rotation of the

ankle may move during the exercises since the ankle is not a perfect spherical articulation). Finally, the sole support has two anchor parts, one for the toes and the second for the heel.

VI. KINEMATIC SIMULATION

A numerical simulation has been performed based on the kinematic models derived in Section IV (using the Matlab software [17]) where a set of six consecutive values were defined as inputs for the joint angles resulting in a set of motions defined by physical therapists, to generate simple and combined motions for the lower limb. Between each two sets of intermediary points the robot would stop to enable a better evaluation of each component and the correspondence between the angular values and the motion at the level of the active joints. Table 4 presents the joint angles used in the simulation. As geometric and motion parameters, the following equation introduces the numerical values used which

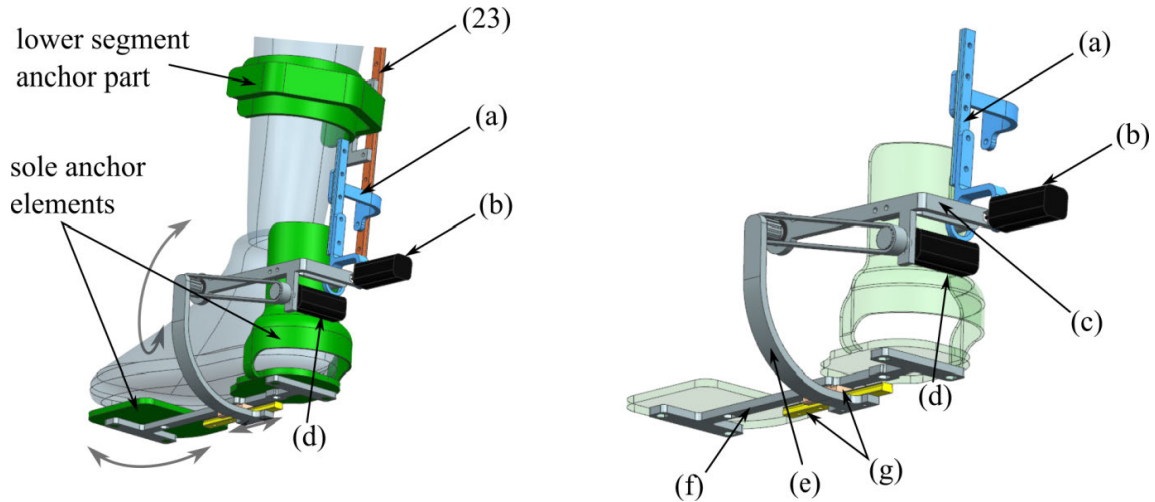


FIGURE 13. RAISE ankle rehabilitation module (CAD representation).

TABLE 4. The input data for the simulation software.

Joint angle	Motion steps expressed in degrees [°]					
	Step 1	Step 2	Step 3	Step 4	Step 5	Step 6
α_{hip_v}	0	45	45	30	20	0
α_{hip_l}	0	0	5	10	5	0
α_{knee}	0	0	-30	-10	0	0
α_{ank_v}	0	0	0	0	20	0
α_{ank_l}	0	0	0	0	15	0

correspond to a person with a height of 180 cm.

$$\begin{aligned}
 l_1 &= 390 \text{ [mm]}, & l_2 &= 190 \text{ [mm]}, \\
 L_{high} &= 550 \text{ [mm]}, \\
 L_0 &= 265 \text{ [mm]}, & L_{leg} &= 530 \text{ [mm]}, \\
 L_{angle} &= 380 \text{ [mm]}, \\
 L_B &= 520 \text{ [mm]} \\
 v_{max_hip} &= 5 \text{ [}^\circ/\text{s]}, & v_{max_knee} &= 4 \text{ [}^\circ/\text{s]}, \\
 v_{max_ankle} &= 3 \text{ [}^\circ/\text{s]} \\
 a_{hip} &= 10 \text{ [}^\circ/\text{s}^2], & a_{knee} &= 8 \text{ [}^\circ/\text{s}^2], \\
 a_{ankle} &= 6 \text{ [}^\circ/\text{s}^2] & & (22)
 \end{aligned}$$

The motion is numerically simulated, using the kinematic equations determined before, with a break between each step (where the motion speed is reset to zero). Figure 14 illustrates angular displacements, speeds and accelerations at the level of the joints while Figure 15 illustrates the corresponding values for the active joints of the robot.

VII. DISCUSSION

It is widely understood that the kinematics of the anatomic joints are more complicated than simple revolute or spherical joints used in mechanism science (e.g. methods for the kinematic modeling for the knee are presented in [3]). For the robotic assisted rehabilitation one challenge is to develop

robotic systems that comply with the kinematic requirements of the limb (either through mechanical design or through adequate control). Since in the RAISE robotic system there is no fixture between the anchor points and the mechanism (since compliant elements are used in the design) the motion of the anatomic joints will comply with the motion of the kinematic chain of the robot (which mounts the lower limb). Consequently, the simple design of the RAISE robotic system should still be capable to perform the rehabilitation exercises in a safe and efficient manner, with the advantages of modularity, simplicity of design and lower implementation cost.

Precision is not critical for the rehabilitation exercises (knowing the joint angle displacement is less important than joint compliance, especially when safety is considered) whereas the proper support of the limb through anchor elements is. In the acute phase, stroke patients may lose muscular tonus and the anatomic joints must be handled carefully. In [5] the authors investigated a cable robot and showed how it should perform for the lower limb rehabilitation. Although the solution has appropriate workspace and a reduced cost of implementation it has only one anchor element (below the knee) whereas RAISE has two anchor elements to control the knee (which, according to the authors' and kineto-therapists' opinion, offers a safer control). Moreover, even if there are rehabilitation clinics that have access to a consecrated device for gait rehabilitation such as LokoHelp [6], Lokomat [22], The Gait Trainer [10], in the acute stroke stages, these robotic systems may not be usable since the patient motor capabilities may be highly affected. A device which allows the early gait rehabilitation of bedridden stroke patients (such as RAISE or the devices ones found in [20], [27]) should offer therapeutic benefits.

Exoskeletons for lower limb rehabilitation were also investigated in the scientific literature. The most predominant mechanical architectures are the serial ones (or the open chain ones such as the RRR rehabilitation exoskeleton in [23]) and the closed loop chain ones (see [7], [8]). The advantage of the

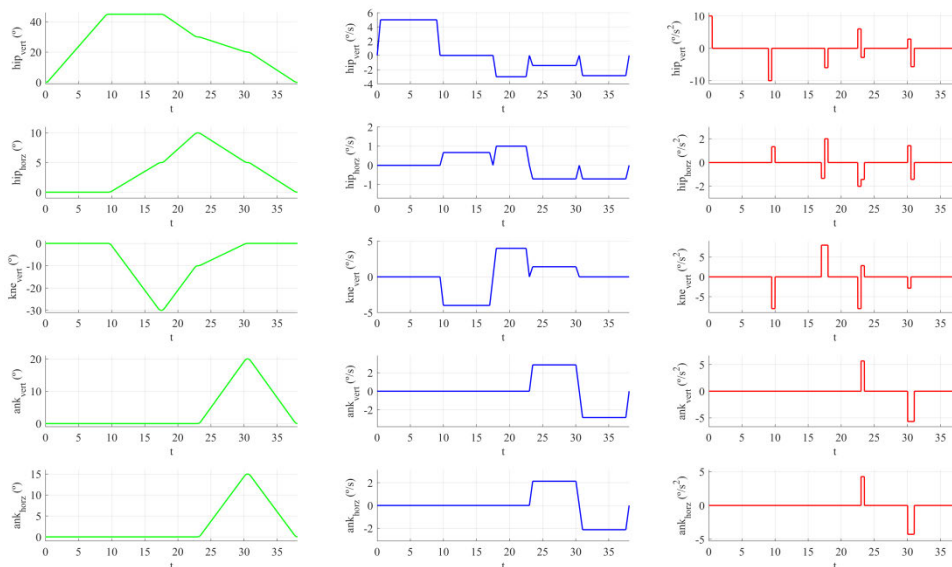


FIGURE 14. The angular displacements, velocities and accelerations at the level of the human joints.

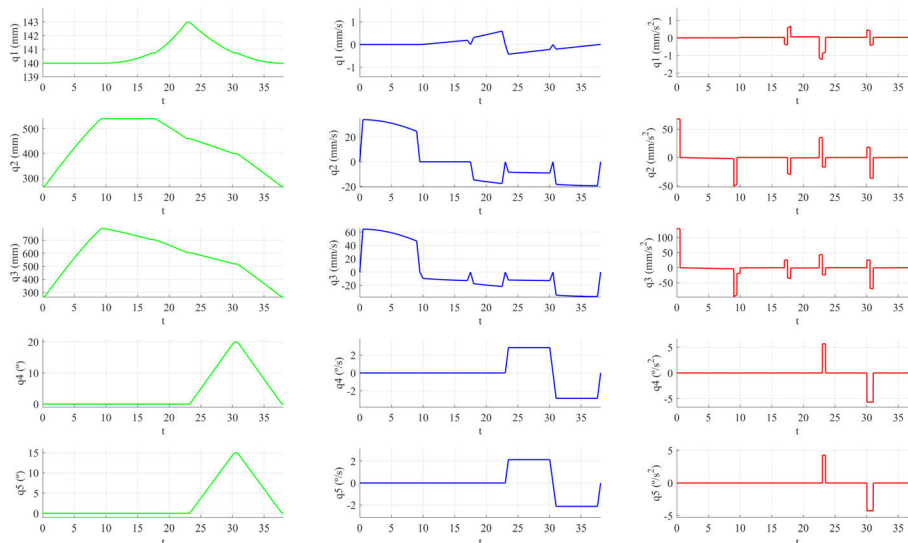


FIGURE 15. The angular displacements, velocities and accelerations at the level of the active joints of the robot.

serial ones is the larger workspace and kinematic simplicity whereas the advantage of the closed loop ones is that the load of the kinematic carried by the kinematic chains is reduced (as opposed to a serial chain where e.g. the base actuator must carry all other actuators). The RAISE robotic system is designed based on a closed loop (parallel) mechanism which reduced the load that the actuators must carry, but it also has a serial spherical mechanism for the ankle joint rehabilitation. Since RAISE is designed for the rehabilitation of the bedridden stroke patients, the emphasis on the ankle mechanism is not required when the load is considered (since the sole of the foot will not touch the floor). Other example of exoskeleton rehabilitation device is found in [24] where the

authors used wire based actuators. However the device does not provide the rehabilitation for the ankle joint.

Analyzing other review papers which classify robotic systems for lower limb rehabilitation [11], [18], [19], [25], [26] the authors did not identified any robotic systems which approach the patient in the way presented in this paper. However, a similar solution (with respect to RAISE robotic system) was found in the literature, the NEURObike [20], which has only 3 DoF working as a planar mechanism, whereas RAISE brings a total of 5 DoF, adding the lateral motions at the level of the hip and ankle. Moreover, a robotic device for lower limb rehabilitation was presented in [27] capable of performing a limb motion for both knee and hip

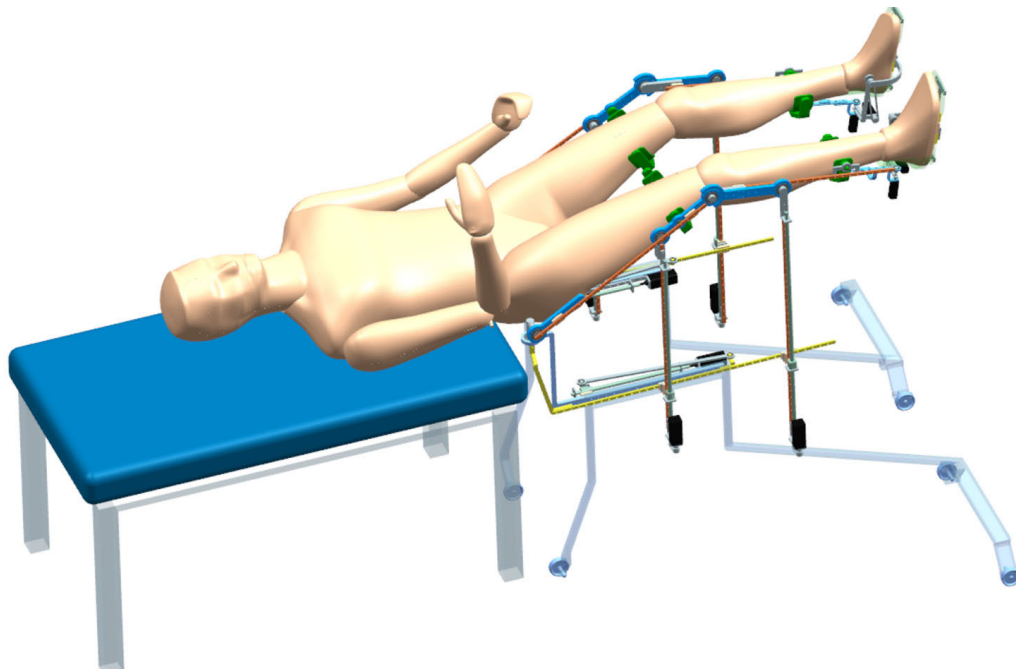


FIGURE 16. CAD model of RAISE in a mirrored configuration attached to a patient.

joints simultaneously. The advantage of the RAISE robotic system over the one in [27] refers to the anchor elements of RAISE (since the robotic system from [27] has only one anchor element at the level of the ankle).

Although the experimental data for the motion amplitude has no significance in evaluating the efficiency of the RAISE robotic system (since it was acquired from healthy patients), it provides relevant information about the operational workspace which in turn helps in developing the mechanical design of the robot. Moreover, in contrast to other motion monitoring solutions (such as optical tracking devices [28] which are harder to mount and calibrate), the biomedical system of sensors (which is medically certified and straightforward to use) used for experiments can be used for the initial evaluation of the patients, the real-time monitoring of the patients during the exercises and for providing a database that can evaluate the progress in time for each subject. In addition, the experiments revealed specific motion particularities where e.g. the hip flexion motion has components in both the sagittal and coronal planes (see figure 6). In order to increase the safety while decreasing the risk of anatomic joint stain, these particularities of the movement should be considered when defining the rehabilitation exercises using RAISE robotic system (or even other robotic systems which are designed for bed ridden patients).

Despite the fact that the RAISE robotic system development is not yet in the evaluation stage for the motor rehabilitation exercises (for patients with neuromuscular disorders), the authors believe that the design is feasible for the rehabilitation exercises. This is due to two main aspects: first, the preliminary numerical results for the rehabilitation exercises show that RAISE is able to manipulate the lower

limb in the defined ranges of motion without entering singular configurations; second, by comparing the RAISE robotic system concept with state of the art systems some specific advantages were pointed (discussed early in the section) which may be summarized as: increased number of controlled DOFs, increased number of anchor elements, operational workspace to allow multiple exercise set-ups and modularity. Moreover, the cost of the robotic system when it reaches a maturity level of TRL 9 (commercial stage), by the authors estimations, should be lower than 150.000 Euros, which according to MAR [2] is one characteristic that defines an efficient rehabilitation device for the lower limb.

RAISE has been designed as a simple robotic system attachable to almost any bed. The solutions for the right and left leg are symmetrical allowing also the use of a dual robot configuration (figure 16). The use of an external system of sensors for both local muscle activity and joints amplitudes and systemic parameters allow the use of any human robot interaction strategies including the mirrored approaches, making the robot usable for all the rehabilitation stages [21], each having specific HRI with medical relevance. The link lengths of RAISE are adaptable allowing the robot to be configured for the patient anthropometric data without any performance hinder.

A 3D scaled mockup (1:5) of the RAISE robotic system (for the right leg) has been achieved using 3D printing technologies, to validate the initial concept (figure 17).

The kinematic approach is different with respect to the classical systems where the mathematical model defines the relation between the active joints and the end-effector coordinates. In this case the kinematics establish simple relationships between the body joints and the robot' actuators

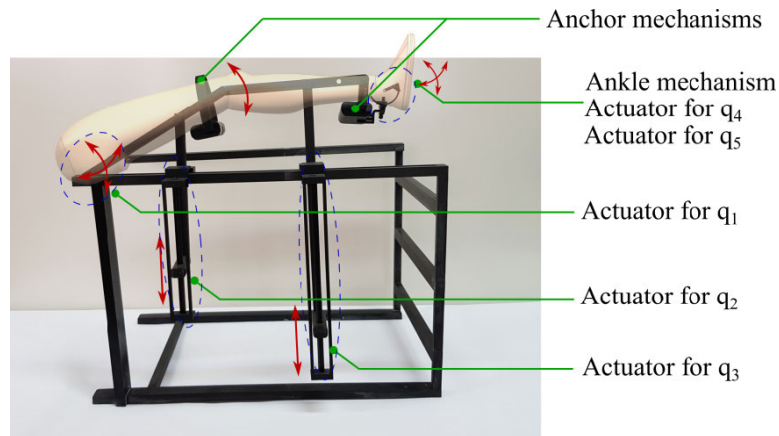


FIGURE 17. 3D scaled mockup (1:5) of RAISE for the right leg.

which allow straightforward programming of any exercises which are defined by amplitude (angular) variations of the articulations. This is true since the kinematics of the robotic system is strongly correlated with the patients' lower limb joint motions (this result regarding the motion parameterization was also discussed in [29]). Some differences may exist between the value of the angle of the patient's joint and the value of the mechanism revolute joint angle (adjacent to the patient limb joint). However, as previously pointed, accuracy is not a priority in the rehabilitation task and this discrepancy may be monitored by the body mounted sensors (e.g. goniometers).

The singularities analysis, validated also in [29] has shown that RAISE can work in a singularity free workspace while providing sufficient motion amplitudes for each body joint. This is also shown numerically for a simulated rehabilitation task. Motions can be achieved individually for each body segment and combined in any possible configuration without interference.

VIII. CONCLUSION

The paper presented the systematic development of an innovative parallel robotic system for the rehabilitation of the lower limb for bed-ridden patients (RAISE). At first the motion amplitudes were determined for each targeted anatomic joints of the lower limb (hip, knee and ankle) by analyzing the motion capabilities of healthy subjects and the experimental data served as a design basis for the robotic system. After a mechanism synthesis, the kinematics, singularities, and operational workspace were determined analytically. Since the operational workspace has only one singularity (which has little effect on the exercises but must be avoided nevertheless) the authors believe that the proposed robotic system should be feasible (safe wise) for the rehabilitation process. Moreover, the RAISE robotic system presents important features which are also desired in robotic rehabilitation (according to kineto-therapists) such as: adequate control points for the anatomic joints, modularity, good usability and compliant mechanism for the limb segments anchor. Numerical simulations were also performed to

initially evaluate the robotic system design, i.e. to determine if it can perform the exercise motions (defined by the experimental data on healthy subjects). The results demonstrate the technical feasibility of the proposed design.

Further work is intended for the prototyping of the RAISE robotic system, evaluating its medical feasibility in a set of clinical trials where all the physiological data relevant to the medical process are taken into consideration (joint angles, motion amplitudes, exerted torques, etc.).

ACKNOWLEDGMENT

The paper presents results from the research activities of the project ID 37_215, MySMIS code 103415 "Innovative approaches regarding the rehabilitation and assistive robotics for healthy ageing" co-financed by the European Regional Development Fund through the Competitiveness Operational Programme 2014–2020, Priority Axis 1, Action 1.1.4, through the financing contract 20/01.09.2016, between the Technical University of Cluj-Napoca and ANCSI as Intermediary Organism in the name and for the Ministry of European Funds.

REFERENCES

- [1] V. L. Feigin, M. H. Forouzanfar, and R. Krishnamurthi, "Global burden of diseases, injuries, and risk factors study 2010 (GBD 2010) and the GBD stroke experts group. Global and regional burden of stroke during 1990–2010: Findings from the global burden of disease study 2010," *Lancet*, vol. 383, pp. 245–254, Jan. 2014.
- [2] *Multi-Annual Roadmap for Robotics in Europe*, Robotics, Dec. 2016.
- [3] D. Tarnita, M. Catana, and D. Tarnita, "Contributions on the modeling and simulation of the human knee joint with applications to the robotic structures," in *New Trends in Medical and Service Robots (Mechanisms and Machine Science)*, vol. 20. New York, NY, USA: Springer-Verlag, 2014, pp. 283–297, doi: 10.1007/978-3-319-05431-5_19.
- [4] J. Galvez and D. Reinkensmeyer, "Robotics for gait training after spinal cord injury," *Topics Spinal Cord Injury Rehabil.*, vol. 11, no. 2, pp. 18–33, Oct. 2005.
- [5] G. Carbone, C. C. Arostegui, M. Ceccarelli, and O. Altuzarra, "A study of feasibility for a limb exercising device," in *Proc. 1st Int. Conf. Italy (IFTOMM)*, in *Mechanisms and Machine Science*, vol. 47, 2017, pp. 11–21.
- [6] S. Freivogel, J. Mehrholz, T. Husak-Sotomayor, and D. Schmalohr, "Gait training with the newly developed 'LokoHelp'-system is feasible for non-ambulatory patients after stroke, spinal cord and brain injury. A feasibility study," *Brain Injury*, vol. 22, nos. 7–8, pp. 625–632, Jan. 2008.

- [7] C. Copilusi, M. Ceccarelli, and G. Carbone, "Design and numerical characterization of a new leg exoskeleton for motion assistance," *Robotica*, vol. 33, no. 5, pp. 1147–1162, Jun. 2015.
- [8] C. Copilusi, M. Ceccarelli, N. Dumitru, and G. Carbone, "Design and simulation of a leg exoskeleton linkage for a human rehabilitation system," in *Proc. 2nd Conf. Mech., Transmiss. Appl.*, vol. 17, 2014, pp. 117–125.
- [9] Y. Sankai, "Hybrid Assistive Limb based on cybernics," *J. bionic Eng.*, vol. 3, pp. 25–34, 2011.
- [10] H. Schmidt, C. Werner, R. Bernhardt, S. Hesse, and J. Krüger, "Gait rehabilitation machines based on programmable footplates," *J. Neuroeng. Rehabil.*, vol. 4, no. 1, p. 2, Dec. 2007.
- [11] I. Díaz, J. J. Gil, and E. Sánchez, "Lower-limb robotic rehabilitation: Literature review and challenges," *J. Robot.*, vol. 2011, pp. 1–11, Nov. 2011.
- [12] D. Tarnita, I. Geonea, A. Petcu, and D. N. Tarnita, "Numerical simulations and experimental human gait analysis using wearable sensors," in *New Trends in Medical and Service Robots (Mechanisms and Machine Science)*, vol. 48, M. Husty and M. Hofbaur, Eds. Cham, Switzerland: Springer, 2018, pp. 289–304.
- [13] K. A. Major, Z. Z. Major, G. Carbone, A. Pisla, C. Vaida, B. Gherman, and D. L. Pisla, "Ranges of motion as basis for robot-assisted post-stroke rehabilitation," *HVM Bioflux*, vol. 8, no. 4, pp. 192–196, 2016.
- [14] C. Vaida, I. Birlescu, A. Pisla, G. Carbone, N. Plitea, I. Ulinici, B. Gherman, F. Puskas, P. Tucan, and D. Pisla, "Raise—An innovative parallel robotic system for lower limb rehabilitation," in *Proc. MESROB New Trends Med. Service Robot.*, Rome, Italy, 2018, pp. 293–302.
- [15] N. Plitea, C. Vaida, B. Gherman, A. Szilaghyi, B. Galdau, D. Cocorean, F. Covaciu, and D. Pisla, "Structural analysis and synthesis of parallel robots for brachytherapy," in *New Trends in Medical and Service Robots (Mechanisms and Machine Science)*, vol. 16. Cham, Switzerland: Springer, 2014, pp. 191–204.
- [16] J. P. Merlet, *Parallel Robots*, 2nd ed. Amsterdam, The Netherlands: Springer, 2006.
- [17] *MathWorks Matlab*. Accessed: May 11, 2019. [Online]. Available: <https://www.mathworks.com/products/matlab.html>
- [18] N. Koceska and S. Koceski, "Review: Robot devices for gait rehabilitation," *Int. J. Control Automat.*, vol. 62, no. 13, pp. 1–8, Jan. 2013.
- [19] X. Zhang, Z. Yue, and J. Wang, "Robotics in lower-limb rehabilitation after stroke," *Behav. Neurol.*, vol. 2017, Art. no. 3731802, Jun. 2017, doi: [10.1155/2017/3731802](https://doi.org/10.1155/2017/3731802).
- [20] V. Monaco, G. Galardi, J. H. Jung, S. Bagnato, C. Boccagni, and S. Micera, "A new robotic platform for gait rehabilitation of bedridden stroke patients," in *Proc. IEEE Int. Conf. Rehabil. Robot.*, Jun. 2009, pp. 383–388, doi: [10.1109/ICORR.2009.5209548](https://doi.org/10.1109/ICORR.2009.5209548).
- [21] C. Vaida, G. Carbone, K. Major, Z. Major, N. Plitea, and D. Pisla, "On human robot interaction modalities in the upper limb rehabilitation after stroke," *Acta Technica Napocensis, Appl. Math., Mech., Eng.*, vol. 60, no. 1, pp. 1–12, 2017.
- [22] S. Jezernik, G. Colombo, T. Keller, H. Frueh, and M. Morari, "Robotic orthosis Lokomat: A rehabilitation and research tool," *Neuromodulation, Technol. Neural Interface*, vol. 6, no. 2, pp. 108–115, Apr. 2003.
- [23] J. Veneman, R. E. Kruidhof Hekman, R. Ekkelenkamp, E. Van Asseldonk, and H. van der Kooij, "Design and evaluation of the LOPES exoskeleton robot for interactive gait rehabilitation," *IEEE Trans. Neural Syst. Rehabil. Eng.*, vol. 15, no. 3, pp. 379–386, Sep. 2007.
- [24] L. Xie and L. Huang, "Wirerope-driven exoskeleton to assist lower-limb rehabilitation of hemiplegic patients by using motion capture," *Assembly Autom.*, Apr. 2019, doi: [10.1108/AA-11-2018-0221](https://doi.org/10.1108/AA-11-2018-0221).
- [25] A. Esquenazi and M. Talaty, "Robotics for lower limb rehabilitation," *Phys. Med. Rehabil. Clinics North Amer.*, vol. 30, no. 2, pp. 385–397, May 2019.
- [26] J. Moreno, J. Figueiredo, and J. Pons, "Exoskeletons for lower-limb rehabilitation," in *Rehabilitation Robotics*. 2018, ch. 7, pp. 88–99. [Online]. Available: <https://books.google.ro/books?id=xuDWDgAAQBAJ&printsec=frontcover#v=onepage&q&f=false>
- [27] N. J. Berezny, D. Dowlatshahi, and M. Ahmadi, "Novel concept of a lower-limb rehabilitation robot targeting bed-bound acutestroke patients," in *Proc. 42nd Conf. Can. Med. Biol. Eng. Soc.*, May 2019, p. 42.
- [28] *OptiTrack*. Accessed: Dec. 2019. [Online]. Available: <https://www.optitrack.com/>
- [29] M. Husty, I. Birlescu, P. Tucan, C. Vaida, and D. Pisla, "An algebraic parameterization approach for parallel robots analysis," *Mechanism Mach. Theory*, vol. 140, pp. 245–257, Oct. 2019.
- [30] P. Tucan, B. Gherman, K. Major, C. Vaida, Z. Major, N. Plitea, G. Carbone, and D. Pisla, "Fuzzy logic-based risk assessment of a parallel robot for elbow and wrist rehabilitation," *Int. J. Environ. Res. Public Health, Appl. Robot. Devices Neurol. Rehabil.*, vol. 17, no. 2, p. 654, Jan. 2020.



CALIN VAIDA was born in Cluj-Napoca, Romania, in 1980. He received the B.S. and M.S. degrees in industrial robotics, in 2003, and the Ph.D. degree in mechanical engineering, in 2009, from the Technical University of Cluj-Napoca.

From 2009 to 2014, he was a Lecturer with the Technical University of Cluj-Napoca, where he is currently an Associate Professor. Since 2005, he has been a Researcher within CESTER (Research Center for Industrial Robots Simulation and Testing), where his activity focused on the development of parallel robots for medical applications. He is the author of three books, over 150 articles, and ten patent applications, being involved in more than 15 research grants with national or international funding. His research interests cover parallel robots kinematics, biomedical engineering, and mathematical and numerical modeling and simulation.



IOSIF BIRLESCU was born in Brasov, Romania, in 1986. He received the B.S. degree in optometry from the Transilvania University on Brasov, Romania, in 2012, and the M.S. degree in biomedical engineering sciences from the University of Applied Sciences, Technikum Wien, Austria, in 2015. He is currently pursuing the Ph.D. degree with the Technical University of Cluj-Napoca.

He is working as a Research Assistant with CESTER (Research Center for Industrial Robots Simulation and Testing), Technical University of Cluj-Napoca, where his activity is focused on development of parallel robots and devices for surgical and oncological applications. His research interests include kinematic modeling methods for parallel robots and design of medical instruments.



ADRIAN PISLA was born in Sibiu, Romania, in 1962. He received the B.S. and M.S. degrees in machine-tools from the Technical University of Cluj-Napoca, in 1987, and the Ph.D. degree in industrial engineering, with double supervision, from the Technical University of Cluj-Napoca and the IPA Fraunhofer Institute, Stuttgart, Germany.

Since 2003, he has been a Full Professor and a Ph.D. Supervisor with the Technical University of Cluj-Napoca. He is currently working as a Senior Researcher with CESTER (Research Center for Industrial Robots Simulation and Testing), coordinating the Dynamic System Simulation Laboratory. He published over 100 scientific articles and ten books, and participating in over 30 national and international research grants. His research interests include the development and integration of robotic system in industrial applications, including the aerospace field and PLM—Product Lifecycle Management.



IONUT-MIHAI ULINICI was born in Borsa, Romania, in 1994. He received the B.S. degree in industrial robotics from the Technical University of Cluj-Napoca, in 2017, where he is currently pursuing the M.S. degree, with the thesis being due to be presented in the summer of 2019.

Since 2017, he has been working as a Research Assistant within CESTER (Research Center for Industrial Robots Simulation and Testing), where his activity is focusing on the development of robotic devices for the post stroke rehabilitation of the upper and lower limb. He is the coauthor of four articles and one patent application, being involved in one EU funded research project. His research interests include parallel robots, and medical robotic devices and simulation.



DANIELA TARNITA was born in Craiova, Romania, in 1959. She received the degree in engineering and the degree in economics from the University of Craiova, in 1982 and 1995, respectively, and the Ph.D. degree in engineering sciences.

Since 1984, she has been teaching at the University of Craiova. In 2001, she became a Full Professor in biomechanics; mechanisms theory and strength of materials. In 2007, she has coordinated Ph.D. students in the field of biomechanics and biomedical engineering. She is the Head of the Biomechanics Laboratory, INCESA Research Centre, University of Craiova, and the Head of the Research Centre in Mechanical Engineering, University of Craiova. She has been the Head of the Doctoral School in Mechanical Engineering, University of Craiova, for four years. She has published more than 165 articles, among which 77 ones are included in ISI journals, ISI proceedings, and BDI journals, 14 books, and 18 book chapters. She currently holds six patents in the field of medicine. Her scientific research activities include biomechanics, robotics, numerical simulations, and analyses with finite element method in biomechanics, intelligent materials and their medical applications, design and optimizing of orthopedic implants and of rehabilitation devices, experimental evaluations of human movements, and nonlinear dynamics of human movement. She has been awarded the title of Doctor in Engineering Sciences.



DOINA PISLA was born in Cluj-Napoca, Romania, in 1968. She received the degree (Hons.) in industrial engineering from the Technical University of Cluj-Napoca, in 1991, and the Ph.D. degree, in 1997.

She became a Full Professor in computer programming and parallel robots, in 2005. Since 2007, she became a Ph.D. Supervisor, coordinating multiple theses on topics covering the development of innovative parallel robotic structures for medical applications. In 2001, she founded CESTER Research Center which became one of the most representative research structures of the Technical University of Cluj-Napoca. Since 2017, she has been the Director of the Council of Doctoral Studies. She published over 180 scientific articles and eight books, being involved in over 30 national and international projects which led to over ten patent applications. Her research interests include robotics and mechatronics, computer and simulation techniques, kinematics and dynamics of serial and parallel robots, mini- and microrobots, biomedical engineering, e-learning platforms, and simulators for medicine. She coordinated the TC in Computational Kinematics of IFToMM for four years.

...



GIUSEPPE CARBONE was born in Salerno, Italy, in 1972. He received the master's degree (*cum laude*) and the Ph.D. degree from the University of Cassino, Italy, where he is being a key member of the Laboratory of Robotics and Mechatronics (LARM) for about 20 years.

From 2015 to 2017, he was a Senior Lecturer with Sheffield Hallam University, U.K., and a member of the executive board of Sheffield Robotics. Since 2019, he has been an Associate Professor with DIMEG, University of Calabria, Italy. He edited/co-edited four books with Springer International Publisher. He has been participating or coordinating more than 20 research projects at national and international level, including 7th European Framework and Horizon 2020. His research interests include aspects of mechanics of manipulation and grasp, mechanics of robots, and mechanics of machinery with more than 300 published articles and over ten patent submissions. He has received several awards, including three IFToMM "Young Delegate" Awards and two JSPS Awards in Japan. He is currently the Deputy Chair of IFToMM Technical Committee on Robotics and Mechatronics, the Deputy Chair of the Youth Committee of the Society of Bionics and Biomechanics, and a Treasurer of the IFToMM Italy Society.